Gigantic eruption of a Carpathian volcano marks the largest Miocene transgression of Eastern Paratethys

Article *in* Earth and Planetary Sciences Letters · June 2021

DOI: 10.1016/j.epsl.2021.116890

CITATIONS
0

READS
209

10 authors, including:

Martin Danisik
Curtin University
187 PUBLICATIONS **2,875** CITATIONS
SEE PROFILE

Vera Ponomareva
Institute Of Volcanology And Seismology
142 PUBLICATIONS **2,539** CITATIONS
SEE PROFILE

Maxim Portnyagin
261 PUBLICATIONS **3,776** CITATIONS
SEE PROFILE

Andrei Zastrozhnov
A.P. Karpinsky Russian Geological Research Institute
27 PUBLICATIONS **263** CITATIONS
SEE PROFILE

Earth and Planetary Science Letters 563 (2021) 116890

Contents lists available at ScienceDirect

Earth and Planetary Science Letters

www.elsevier.com/locate/epsl

Gigantic eruption of a Carpathian volcano marks the largest Miocene transgression of Eastern Paratethys

Martin Danišík [a,*], Vera Ponomareva [b], Maxim Portnyagin [c,d], Sergey Popov [e], Andrei Zastrozhnov [f], Christopher L. Kirkland [a], Noreen J. Evans [a], Evgeny Konstantinov [g], Folkmar Hauff [c], Dieter Garbe-Schönberg [h]

[a] John de Laeter Centre/School of Earth and Planetary Sciences, Curtin University, Perth, WA 6845, Australia
[b] Institute of Volcanology and Seismology, Piip Boulevard 9, Petropavlovsk-Kamchatsky, 683006, Russia
[c] GEOMAR Helmholtz Centre for Ocean Research Kiel, Wischhofstrasse 1-3, 24148, Kiel, Germany
[d] V.I. Vernadsky Institute of Geochemistry and Analytical Chemistry, Kosygin St. 19, Moscow, 119991, Russia
[e] Borissiak Paleontological Institute, Profsoyuznaya Str., 123, Moscow, 117647, Russia
[f] Karpinsky Russian Geological Research Institute (VSEGEI), 74 Sredny Prospect, St. Petersburg, 199106, Russia
[g] Institute of Geography, Staromonetniy Lane. 29, Moscow, 119017 Russia
[h] Institute of Geosciences, Kiel University, Ludewig-Meyn-Strasse 10, 24118, Kiel, Germany

ARTICLE INFO

Article history:
Received 12 December 2020
Received in revised form 8 March 2021
Accepted 12 March 2021
Available online xxxx
Editor: R. Hickey-Vargas

Keywords:
zircon double-dating
(U-Th)/He
U-Pb
tephrochronology
Gorelka tephra
Eastern Paratethys

ABSTRACT

Volcanic ash layers (tephras) dispersed over large areas may offer important time markers in the geological record provided their age and geochemical fingerprint can be established. Accurately dated and geochemically characterized tephras are essential in correlation of temporally and spatially discontinuous geological records, which is key for paleoenvironmental, paleoclimatic, and paleogeographic reconstructions. Here we report geochronological and geochemical data for the Gorelka tephra (southwestern Russia) – a prominent tephra of uncertain age and origin that provides a key time marker for the largest marine transgression of the Eastern Paratethys Sea in the Miocene. Coupled U-Pb and (U-Th)/He dating of zircon crystals constrains the eruption age of the Gorelka tephra, and hence the age of the highest stand of Eastern Paratethys in the Miocene, to 11.5±0.5 Ma. Geochemical characteristics in combination with the new eruption age and tephra volume estimates suggest a magnitude ~7.4 eruption from a volcanic source in the Transcarpathian region. The Gorelka tephra was transported ~1,500 km ENE from its source by westerly winds, which were typical for the atmospheric circulation regime within the Ferrel cell in Central Europe during Sarmatian times. Based on the results presented here, the Gorelka tephra provides a reliable tie-point for paleoenvironmental and stratigraphic correlations across southeastern Europe.

1. Introduction

Volcanic ash beds (tephras) dispersed over significant areal extent (thousands of km^2) provide important isochronous stratigraphic markers that can be used to date events in both geological and human history. Such deposits provide key markers that correlate geographically discontinuous geological records, which is critical to a wide range of paleoenvironmental, paleoclimatic, paleogeographic, and stratigraphic questions (e.g., Lowe, 2011). A robust tephra time marker requires accurate eruption age and mineralogical/geochemical characterization to allow fingerprinting. However, accurate and precise dating of tephras is not always straightforward given the common lack of datatable material or limited accessibility to viable dating methods. Given these challenges, the chronology of many important tephras remains disputed (e.g., Danišík et al., 2020).

The Gorelka tephra, a prominent layer of white volcanic ash of enigmatic origin found in a paleovalley of the Don River near Gorelka Village in southwestern Russia (Fig. 1), intercalates a sequence of marine deposits, interpreted to have formed during the largest Miocene marine transgression of the Eastern Paratethys (Iosifova, 1977; Iosifova et al., 1986; Popov et al., 2004. During this maximum transgression (mapped by the spatial distribution of marine sediments and paleo-shorelines), the Paratethys Sea covered the lowlands on the southern edge of the East European Plain and intruded the paleo-Don valley, advancing upstream for some ~450 km (Iosifova, 1977; Iosifova et al., 1986; Popov et al., 2004). The Gorelka tephra thus marks an important paleoenvironmental

* Corresponding author.
E-mail address: m.danisik@curtin.edu.au (M. Danišík).

https://doi.org/10.1016/j.epsl.2021.116890
0012-821X/

Fig. 1. A. Simplified physical geography map of SE Europe-SW Asia with the position of Gorelka site and the Don River. The Black, Azov, Caspian and Aral Seas represent the relicts of the Eastern Paratethys Sea. Inset illustrates the position of the area in Eurasia (orange outline). Abbreviations: Carpathian Mts. – Carpathian Mountains; Manych D. – Manych Depression; Azov S. – Azov Sea; Aral S. – Aral sea. **B.** Outcrop of the Miocene deposits with white 2.2 m thick layer of the Gorelka tephra. A black dashed rectangle shows the position of Fig. 1C. Note a person (highlighted in the white outlined ellipse) in the upper right corner for scale. **C**. The lower part of the tephra layer; position and labels of the samples is indicated with red circles and black numbers, respectively. An additional photograph of the Gorelka tephra is provided in Supplementary Figure S1. (For interpretation of the colours in the figure(s), the reader is referred to the web version of this article.)

and stratigraphic boundary and, if dated accurately and geochemically characterized, could provide a temporal constraint on the Eastern Paratethys major marine transgression and serve as an important tie-point for paleoenvironmental and stratigraphic reconstructions across southeastern Europe.

The age of the Gorelka tephra is controversial and its volcanic source hitherto unknown. The Gorelka ash was deposited into green silts and clays with marine and brackish water diatom species, indicating a shallow sea environment (Iosifova, 1977, 1992). Based on paleobotanical and sedimentological data, the bracketing marine deposits to the tephra are identified as middle Sarmatian (ca. 11 Ma; Iosifova, 1977; Yakobovskaya and Iosifova, 1968). In contrast, K-Ar and fission-track dating of the volcanic glass from the tephra yielded ages of 23±5 Ma (Iosifova, 1992) and 19.9±1.4 Ma, respectively, suggesting an early Miocene age (Chumakov et al., 1992). These dates correspond to a marine regression stage of the Paratethys and thus would contradict interpretations of transgressive-regressive cyclicity as argued by Popov et al. (2010), on the basis of lithofacies analysis. Consequently, the Gorelka deposits have not been used to delimit the extent of the largest Miocene Eastern Paratethys marine transgression (Vinogradov, 1967–1969; Popov et al., 2010).

To place accurate temporal constraints on the Miocene marine transgression, this work aims to constrain the eruption age of the Gorelka tephra using a combination of two independent dating techniques – U-Pb and (U-Th)/He dating, both techniques applied on individual zircon crystals. In addition, in order to facilitate application of the Gorelka tephra as a regional correlation marker, we report major and trace element glass chemistry and bulk tephra Sr-Nd-Pb isotopic composition, and, finally, use the new age and geochemistry data to identify the potential volcanic source of the Gorelka tephra and derive some paleoenvironmental inferences.

2. Geological setting

2.1. Sample site

The Gorelka outcrop (N 51.440755° E 42.668847°) is located in the Peschany ("Sandy") ravine near Gorelka village within a Miocene paleovalley of the Don River (Fig. 1). The top of the ~30 m high outcrop has an elevation 142 m above modern sea level. A ~70 m long lens of the white Gorelka tephra lies within a Miocene marine sequence of greenish sands, silts, and clays, overlying eroded early Cretaceous glauconitic sands (Fig. 1B; Iosifova, 1977). The tephra exhibits a sharp contact with the underlying silts and comprises a 0.2 m thick bottom layer overlain by a 2 m thick package of layered ash. Layering in the lower part of the tephra is accentuated by thin rusty crusts reflecting oxidation of iron minerals (Fig. 1C; Supplementary Figure S1). The lower 0.2 m, fine to very fine ash layer likely represents the original tephra fall, while in places the upper ash layer exhibits slumping or oblique layering and likely represents a redeposited unit. The Gorelka tephra and overlying layers were deposited during a reversed polarity paleomagnetic interval (Iosifova, 1992). Lithologically comparable ash at the same stratigraphic interval (thickness of 0.45 m) is also found 6 km north of the Gorelka site (Iosifova, 1977).

2.2. Significance for Eastern Paratethys history

Based on the geological setting, dating the Gorelka tephra would place an important temporal constraint on the largest Miocene transgression of the Eastern Paratethys – a large inland sea that once stretched from the European Alps over Central and Eastern Europe to the Aral Sea and Kopetdagh in western Asia (Fig. 2A). Modern relicts of the Eastern Paratethys include the Black, Azov, Caspian, and Aral seas (Fig. 1A). During Oligocene-Miocene time, the Eastern Paratethys had a restricted connection to the World Ocean with the northern boundary of this basin extending from southern Ukraine to the Northern Azov – Manych – Pre-Caspian Depression to Northern Aral Sea (Figs. 1 and 2).

Eastern Paratethys underwent a series of transgressions and regressions, the age and extent of which are not well constrained. Located on a stable platform, the northern shelf of Eastern Paratethys is in many places represented by shallow marine deposits, which are difficult to directly date. Approximate age estimates for Oligocene-Miocene marine transgressions were obtained by correlation with the Mediterranean realm and from rare, often contradictory radiometric data (Chumakov et al., 1992). The chronostratigraphy of Eastern Paratethys has only recently been constrained by phytoplankton and paleomagnetic data (Popov et al., 2018). The well-preserved Gorelka tephra at the investigated site thus provides a perhaps unique opportunity to date enclosing deposits accumulated under the influence of the advancing Paratethys Sea and hence, constrain the age of the largest Miocene marine transgression.

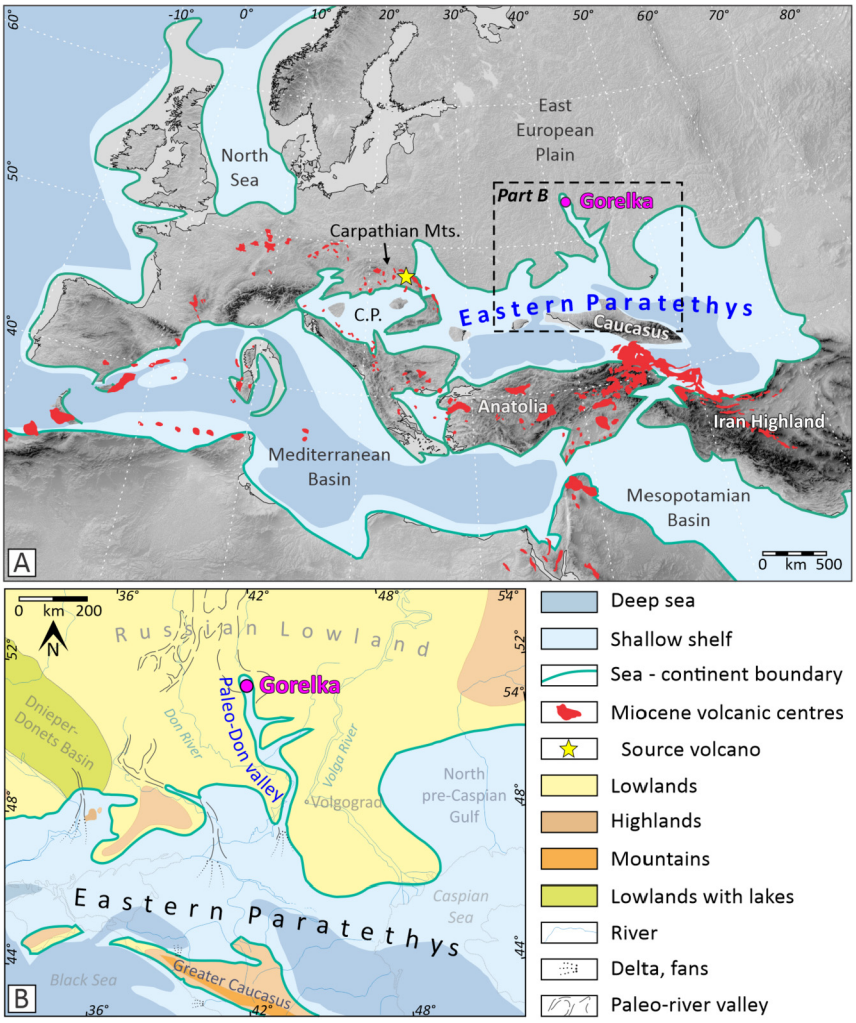

Fig. 2. A. The Mediterranean and Paratethys realms and their major basins and straits during middle Sarmatian times, as inferred from the distribution of middle Sarmatian sediments and faunistic data (modified after Popov et al., 2004). The Eastern Paratethys reached its maximum extent in the Miocene during this time. Cenozoic volcanic fields active in the Miocene (red patches) are shown for circum-Mediterranean and Caucasian-Iran fields according to Lustrino and Wilson (2007) and Dilek et al. (2010), respectively. Magenta circle shows the position of the Gorelka site in the Don River paleovalley; yellow star indicates approximate location of the suggested source volcano; C.P. – Central Paratethys. **B**. Paleogeographic map of northern shoreline of the Eastern Paratethys during the highest stand of the middle Sarmatian transgression (modified after map 7 in Popov et al., 2004). Note that the up to 450 km long and 100 km wide northwards ingression along the Paleo-Don valley was not considered as a part of the Eastern Paratethys due to the existing age discrepancy of Gorelka sediments (Popov et al., 2010).

3. Samples and methods

Three samples of ash were collected from a cleaned section of outcrop (Fig. 1B). Individual glass shards from all three samples were analysed for major element content (51 analyses) and those from one sample were analysed for trace elements (eight analyses); a split of the sample from the upper part of the tephra (marked 8.5 in Fig. 1B), was used for U-Pb and (U-Th)/He geochronology and Sr-Nd-Pb isotope analysis.

Combined dating of zircon by U-Pb and (U-Th)/He methods was carried out at the John de Laeter Centre at Curtin University (Perth, Australia) and is detailed in the Supplementary materials. In brief, separated zircon was mounted in epoxy resin, ground to half-width, polished, and imaged by cathodoluminescence (CL). Zircon was then U-Pb dated using laser ablation multi-collector inductively coupled mass spectrometry (LA-MC-ICPMS). Following the U-Pb analysis, zircon crystals that yielded Miocene U-Pb ages were plucked out of the epoxy mount and analysed by the (U-Th)/He method.

Geochemical characterization included electron microprobe (EMP) and laser ablation inductively coupled mass spectrometric (LA-ICPMS) analyses of volcanic glass for major and trace element composition as described in Portnyagin et al. (2020). Bulk tephra analysis was obtained by thermal ionization mass spectrometry (TIMS) for Sr-Nd-Pb isotope composition.

4. Results

4.1. Geochronology

In total, U-Pb geochronology was undertaken on 40 zircon crystals (Supplementary Table S1). U-Pb ages range from ca. 11 Ma to ca. 3300 Ma. Twenty-six dates define a young component in the range of 11.2±0.2 Ma to 13.8±0.2 Ma (Middle Miocene; uncertainties here and elsewhere reported at 2σ level unless otherwise stated) but do not yield a statistically valid single age component. To identify the youngest coherent age component, we applied the TuffZirc age algorithm (Ludwig and Mundil, 2002). The algorithm was designed to extract reliable U-Pb ages from Phanerozoic tuffs. This is achieved by (i) rejecting the data with anomalously high uncertainties, (ii) ranking of the remaining data and finding the largest cluster of U-Pb ages that yields a probability-of-fit of >0.05. The algorithm then finds the median age of the largest cluster, which is taken as the age closest to the eruption that produced

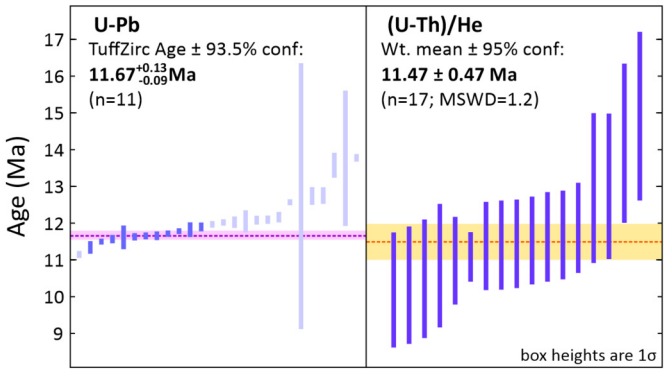

Fig. 3. Ranked order plots of U-Pb and (U-Th)/He datasets; dark blue bars indicate data considered for calculation of the mean ages. Note that U-Pb age provides maximum eruption age (purple dashed line and magenta bar) and this age overlaps within uncertainty with (U-Th)/He age estimate (orange dashed line and deep yellow bar), which directly dates the time of eruption.

the tuff (Ludwig and Mundil, 2002). The TufZirc algorithm applied to the Gorelka zircon U-Pb data yielded an age of 11.7±0.1 Ma (93.5% confidence interval) based on a coherent group of 11 ^{207}Pb corrected U-Pb ages (Fig. 3).

The young zircon age component is represented by euhedral, elongate, prismatic crystals with pyramidal terminations, typical for zircon of volcanic origin (Supplementary Fig. S2A). On the basis of crystal morphology and internal texture, these zircon crystals are interpreted as having been derived from the eruption producing the Gorelka tephra. The remaining zircon crystals with U-Pb ages from 497±7 Ma to 3311±430 Ma are interpreted as inherited and derived from older crustal source regions.

Seventeen crystals from the dominant Miocene U-Pb age population were dated by the (U-Th)/He method. Alpha-ejection corrected (U-Th)/He ages reproduce well, overlap within uncertainty with their corresponding U-Pb ages for all 17 double-dated crystals, and define one unimodal population with a weighted mean age of 11.5±0.5 Ma (95% confidence; n=17; MSWD = 1.2) (Supplementary Table S2).

4.2. Petrography and volcanic glass composition

The Gorelka tephra consists of >95% isotropic colourless volcanic glass (Supplementary Fig. S1B). The majority of glass particles have an elongated angular shape, typical of volcanic pyroclastic material. Pumiceous particles comprise less than 10%. The prevailing size (maximum dimension) of glass shards is 50 to 300 µm. Some particles exhibit signs of secondary alteration expressed by variable electron back scatter response within single shards, whereas unaltered particles are homogeneous. Admixture of host sediments is insignificant.

Gorelka glass is compositionally classified as a homogeneous rhyolite (77-78% SiO_2) with the K_2O contents (3.45-4.51 wt%, median value 3.69 wt%) at the boundary between medium- and high-K rocks (Fig. 4A). Na_2O and K_2O reveal a statistically significant negative correlation (r^2=0.47, n=51), which suggests minor secondary alteration expressed as a complementary depletion in Na and enrichment in K (e.g., Portnyagin et al., 2020). A major population of glass with K_2O <4 wt% comprising ~85% of all analyses, likely reflects the initial glass composition. The other major element abundances do not correlate with alkali abundance and were not affected by alteration. Given the Miocene age of the volcanic ash, preservation of its chemical composition is regarded as exceptionally good.

Trace element compositions were obtained for eight glass shards (Fig. 4B,C), all of which have a similar trace element cargo (Supplementary Table S3). The glasses have relatively high contents of Nb, Y (Y+Nb ~50 ppm), and Rb (~150 ppm) and fall in the middle of the composition field of granites from post-collisional settings, at the compositional boundary between volcanic arc and intra-plate granite magmas (Pearce, 1996; Pearce et al., 1984). A multi-element primitive mantle (PM)-normalized diagram (Fig. 4C) illustrates moderate to strong depletion of Gorelka tephra in Sr, Eu, and Ti, which is typical for many rhyolite magmas. Also noticeable is a Ba depletion relative to Rb and U. Concentrations of heavy rare earth elements and yttrium (HREE+Y) are relatively high (~8×PM), and their normalized pattern is nearly flat (unfractionated). The light and middle rare earth elements (LREE and MREE) are moderately enriched ($[La/Sm]_N$=4.7, where N denotes PM-normalized values). PM-normalized concentrations of Cs, Ba, Rb, Pb, Th and U are strongly elevated compared to Nb, Ta and La, which is distinctive feature of subduction related magmas (Pearce and Peate, 1995). The Nb and Ta contents in the Gorelka tephra are relatively high (~24 ppm and 2 ppm respectively) and exhibit a very modest depletion relative to La.

The Gorelka tephra has a very radiogenic Sr initial ratio ($^{87}Sr/^{86}Sr_{(i)}$=0.70928), moderately radiogenic Pb initial ratio ($^{206}Pb/^{204}Pb_{(i)}$=18.95, $^{207}Pb/^{204}Pb_{(i)}$=15.66, $^{208}Pb/^{204}Pb_{(i)}$=38.90) and unradiogenic Nd initial ratio ($^{143}Nd/^{144}Nd_{(i)}$=0.51247, $\epsilon Nd_{(i)}$= -3.1) (Fig. 4D, Supplementary Table S2). Such isotope Sr-Nd-Pb composition is close to the mantle end-member component of EM-2 (Hofmann, 2003) and intermediate between the composition of the upper mantle (N-MORB in Fig. 4D) and the upper continental crust (Zartman and Haines, 1988).

5. Interpretation and discussion

5.1. Eruption age of the Gorelka tephra

The youngest zircon U-Pb age component in the Gorelka tephra is 11.7±0.1 Ma and this age is interpreted to record the time of magmatic crystallization. This U-Pb age (11.7±0.1 Ma is statistically indistinguishable from the (U-Th)/He age of 11.5±0.5 Ma. The temporal concordance of U-Pb and (U-Th)/He ages demonstrates that crystallization of the Miocene zircon crystals in a magma reservoir (recorded by the U-Pb system) was near contemporaneous with cooling of the zircon below ~200 °C recorded by (U-Th)/He system (e.g., Danišík et al., 2020). This similarity in U-Pb and (U-Th)/He zircon ages is consistent with a geological process that rapidly transferred crystals from magmatic to (near) surface temperatures. Geochronological data from both systems are therefore interpreted to constrain the age of eruption that produced the Gorelka tephra.

Given that (U-Th)/He system should directly date the time of zircon eruption (as opposed to zircon crystallization recorded by U-Pb system), we designate the (U-Th)/He age of 11.5±0.5 Ma as the eruption age of Gorelka tephra despite greater uncertainty relative to the U-Pb age (11.7±0.1 Ma). This newly proposed eruption age is in excellent agreement with the Sarmatian paleobotanical constraint (Iosifova, 1977; Popov et al., 2004), yet demonstrates inaccuracy in the previously published K-Ar and fission track ages. Unfortunately, no information on the analytical procedures nor data quality assessment was provided in these studies (Iosifova, 1977; Chumakov et al., 1992), which precludes further evaluation of the age discrepancy.

5.2. Implications of the new Gorelka tephra age for paleogeography

Our results resolve a longstanding controversy over the age of the Gorelka tephra, previously defined by paleobotanical and sedimentological constraints and K-Ar and fission-track dating (Chumakov et al., 1992). The new date of 11.5±0.5 Ma obtained for the Gorelka tephra suggests a middle Sarmatian (middle Miocene)

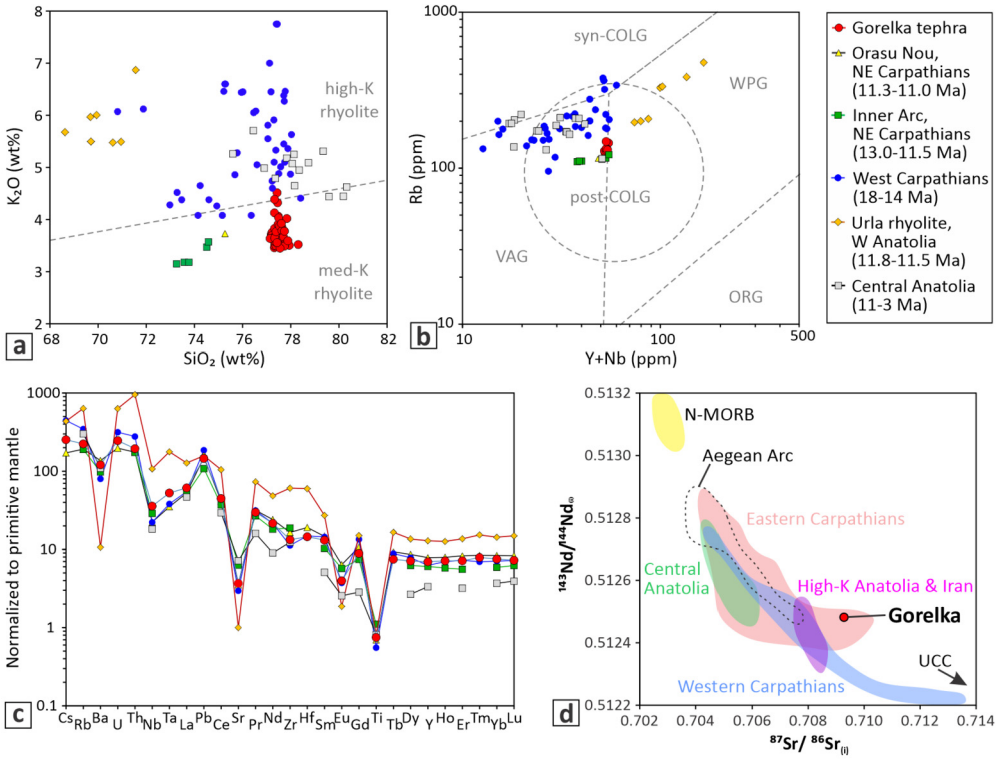

Fig. 4. Major element, trace element, and Sr-Nd isotope composition of Gorelka tephra. (A) K_2O vs. SiO_2 diagram. Dashed lines divide fields of med-K_2O and high-K_2O rhyolites following Le Maitre et al. (2002). (B) Classification (Y+Nb) vs. Rb diagram for granites after Pearce et al. (1984) and Pearce (1996). Dashed lines divide fields of volcanic arc granites (VAG), ocean-ridge granites (ORG), within-plate granites (WPG), syn-collisional granites (syn-COLG), and post-collisional granites (post-COLG). (C) Trace elements normalized to primitive mantle (McDonough and Sun, 1995). (D) Sr-Nd isotope composition of Gorelka tephra in comparison with composition of rocks from the Eastern and Western Carpathians, Aegean Arc (Mason et al., 1996) and Central Anatolia (ignimbrites of Cappadocia; Temel et al., 1998) and middle Miocene high-K rocks from Western Anatolia and Iran (Lechman et al. 2018; Aldanmaz et al., 2000). Bold arrow points to the average composition of the upper continental crust (UCC: $^{87}Sr/^{86}Sr$=0.7149, $^{143}Nd/^{144}Nd$=0.51219; Zartman and Haines, 1988).

age for the enclosing deposits and, for the first time, permits direct temporal constraint on the highest Miocene Eastern Paratethys stand. During this transgression, Eastern Paratethys waters intruded the ~100 km wide paleo-Don valley for ~450 km northwards (Fig. 2B). Thus, the Gorelka tephra can be regarded as an excellent marker for the middle Sarmatian sediments deposited during the maximum transgression of the Eastern Paratethys (Fig. 5).

5.3. Tephra provenance

The volcanic source of the Gorelka tephra is uncertain as the site is located >1000 km from known volcanic areas (Fig. 2A), and the Miocene volcanic record is incomplete. Nonetheless, regions with abundant Miocene volcanism which could be the potential volcanic source for the Gorelka tephra are present in the Anatolia-Iran volcanic belt in the south and Carpathians in the west (Fig. 2A). The precise age obtained in this work, combined with the geochemical and isotopic characterisation, allow us to narrow down the most probable provenance of the Gorelka tephra.

The age of the Gorelka tephra (11.5±0.5 Ma) corresponds closely to the latest collision between the northern edge of Arabia and Anatolia-Caucasus-Pontide margin of Eurasia (Pearce et al., 1990). Beginning from Late Miocene times, abundant post-collisional explosive volcanism occurred in Eastern and Central Anatolia, and in the Caucasus. However, this volcanism mostly post-dates the Gorelka tephra. For example, abundant ignimbrites in Cappadocia in Central Anatolia were erupted between 10 to 2.5 Ma (Le Pennec et al., 2005; Aydar et al., 2012; Lepetit et al., 2014). In addition to the younger age, the Cappadocian ignimbrites are mostly high-K rocks enriched in Rb and relatively depleted in HREE+Y in comparison to the Gorelka tephra, and they have less radiogenic Sr and more radiogenic Nd isotope compositions (Fig. 4D). Similarly, post-collisional volcanism in the Caucasus began at ca. 9 Ma, whereas only sparse volcanic activity occurred there between 9 and 13 Ma (Lebedev et al., 2011; Akal et al., 2013). Some middle Miocene rocks from Iran and Western Anatolia with ages of around 11 Ma, have similar Pb and Nd isotope composition but slightly less radiogenic Sr isotope compositions, in comparison with the Gorelka tephra (Aldanmaz et al., 2000; Helvacı et al., 2009; Akal et al., 2013; Moghadam et al., 2015; Lechmann et al., 2018). However, these rocks are typically less siliceous, strongly enriched in highly incompatible elements and belong to an ultra-high-K series that is geochemically very different from the calc-alkaline rhyolite Gorelka tephra (for example Urla rhyolite from the Western Anatolia; Fig. 4).

Two periods of silicic volcanism occurred in the Carpathians in the Miocene. The first period corresponds to emplacement of the Bükkalja Volcanic Field ignimbrites in northern Hungary (Western Carpathians) at 18.2–14.4 Ma in Badenian time (Lukács et al., 2018). An important tephrostratigraphic marker in the Pannonian Basin (Dej Tuff) was deposited at the end of the first period, at 14.8 ± 0.4 Ma (Szakács et al., 2012; de Leeuw et al., 2013). The Badenian rhyolites are older than the Gorelka tephra and tend to have high-K and relatively low-Nb island arc-like compositions (Fig. 4), although the trace element spectra for Badenian obsidian from the Tokaj Mountains (Rozsa et al., 2006) is similar to that of the Gorelka tephra (Fig. 4C).

A second flare-up of explosive silicic volcanism occurred in the Carpathians during Sarmatian time (between 13.5 and 11 Ma) and was likely related to the volcanic activity in the Transcarpathian region and in the Eastern Carpathians (Pécskay et al., 2000, 2006). Dacite and rhyolite extrusions and tuffs of this age often reach

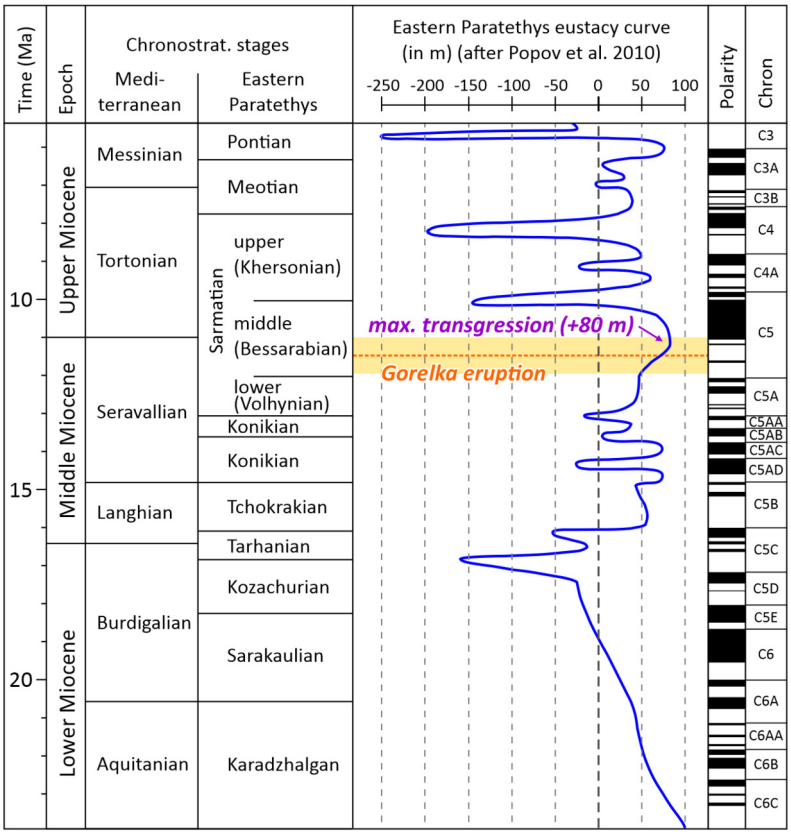

Fig. 5. Comparison of geochronological results with Miocene sea level changes in the Eastern Paratethys. Sea-level fluctuation curve for the Eastern Paratethys (Popov et al., 2010); note the eruption age of the Gorelka tephra overlaps with the maximum transgression phase during the Miocene. Geomagnetic polarity time scale, right side of figure, after Ogg (2020); normal polarity – black, reversed polarity - white.

great thickness and have been described from drill holes near the Hungarian-Ukrainian border in the north-western Pannonian Basin (e.g., ca. 700 m thick rhyolite tuff of Sarmatian age in Gelenéts-1 drill hole, NE Hungary; Pécskay et al., 2000). Similar rocks also crop out in the Tokaj Mountains, Hungary (Kiss et al., 2010), Beregovo region, Ukraine (Seghedi et al., 2001), and at the Orasu Nou volcano (Kovács et al., 2017) and Călimani Mountains (Mason et al., 1998) in Romania. These rhyolites have a slightly lower bulk rock K_2O content relative to the older Badenian rhyolites and they have very similar trace element patterns to volcanic glass in the Gorelka tephra (Fig. 4). Sr-Nd isotope compositions of the Gorelka tephra plot at the high-$^{87}Sr/^{86}Sr$ end of the East Carpathian array and are nearly indistinguishable from some rocks in the Călimani Mountains, Romania (for example, rhyolite #C16 in Mason et al., 1996). The EM-2-like Pb isotope composition of the Gorelka tephra is not very distinctive and overlaps with the compositions of middle Miocene Eastern Carpathian rocks (Mason et al., 1998) as well as those from the Western Anatolia and Iran (Aldanmaz et al., 2000; Lechmann et al., 2018). The distinctive Sr-Nd isotope compositions of the Gorelka tephra and Carpathian silicic rocks suggest strong contamination by continental crust during magma generation (Mason et al., 1998), and in this respect these rocks are different from those of the Central Anatolia and Aegean Arc (Fig. 4D). Thus, based on the similarity of the ages and composition, we propose that the volcanic source of the Gorelka tephra was most likely located in the Transcarpathian or northern Eastern Carpathian region (Fig. 2A).

The distance from the Transcarpathian region to the Gorelka site is ~1,500 km (Fig. 2A). If we assume the original thickness of an ash layer in Gorelka as 0.2 m (the lower massive layer) and a very narrow ~300 km-wide dispersal area, the minimum tephra volume can be estimated at 300 km^3 (based on the single-isopach method of Legros, 2000), which corresponds to an eruption magnitude of ~7.4 (calculated according to Pyle, 1995). This minimum eruption magnitude estimate is close to that for the upper Pleistocene Campanian Ignimbrite (CI tephra), which hitherto, is the only dated tephra marker identified in the East European Plain (e.g., Pyle et al., 2006).

Finally, identification of the volcanic source allows us to make some inferences about paleo-wind directions and climate dynamics. The relative position of the Transcarpathian region and the Gorelka location during Sarmatian times (Fig. 2A) suggests the tephra was transported by an atmospheric current flowing from west (southwest) to east (northeast). This observation fits into the atmospheric circulation model for mid-latitude Central Europe, suggesting that a westerly-dominated wind regime within the Ferrel cell has been established since ~14.5 Ma (Methner et al., 2020) and that westerlies were the prevailing winds in Central Europe in the Sarmatian (Quan et al., 2014).

6. Conclusions

Based on indistinguishable U-Pb and (U-Th)/He ages obtained on a subpopulation of zircon crystals, a new eruption age of 11.5±0.5 Ma is proposed for the Gorelka tephra. The new eruption age constrains the highest stand of the Eastern Paratethys waters during the Miocene to middle Sarmatian times. The Gorelka tephra has a calc-alkaline rhyolite composition, trace element content indicating a post-collisional tectonic setting and EM-2-like Sr-Nd-Pb isotope composition suggesting a large contribution from continental crust into the magma source. These geochemical characteristics, in combination with the newly reported eruption age and tephra volume estimates, indicate a magnitude ~7.4 eruption from a volcanic source in the Transcarpathian region, ~1,500 km WSW from

the Gorelka site. This tephra was transported by westerly winds, typical of the atmospheric circulation regime in Central Europe during Sarmatian times.

Data availability

All data generated or analysed during this study and supporting the findings of this study are included in this published article and its supplementary information files. Supplementary Tables 1-3 contain all data that was used to generate the figures in the main text and in the supplementary files.

CRediT authorship contribution statement

Martin Danišík – designed methodology for geochronological analysis, conducted (U-Th)/He analyses, visualized geochronological data, co-wrote the original draft, acquired funding; Vera Ponomareva – conceptualized the research hypothesis, compiled and translated literature, co-wrote the original draft; Maxim Portnyagin – conceptualized the research hypothesis, conducted geochemical analysis of glass by EPM and LA-ICPMS and analyzed the geochemical data, visualized geochemical data, co-wrote the original draft; Sergei Popov and Andrei Zastrozhnov – provided paleogeography background and drew paleogeography maps; Evgeny Konstantinov – conducted fieldwork and collected samples; Chris Kirkland and Noreen Evans – conducted LA-ICPMS analyses of zircon, edited manuscript; Folkmar Hauff – performed TIMS analyses; Dieter Garbe-Schönberg – managed LA-ICPMS analyses of glass. All co-authors contributed to data interpretation in their respective fields of expertise and provided critical revision to the manuscript.

Declaration of competing interest

The authors declare that they have no known competing financial interests or personal relationships that could have appeared to influence the work reported in this paper.

Acknowledgements

MD was supported by the AuScope NCRIS2 program, Australian Research Council (ARC) Discovery funding scheme (DP160102427) and a Curtin Research Fellowship (CRF170135). This study was enabled by AuScope (auscope.org.au) and the Australian Government via the National Collaborative Research Infrastructure Strategy. The NPII multi-collector used in this work was obtained via funding from the ARC LIEF program (LE150100013). Part of this research was undertaken using SEM instrumentation supported by ARC LE0775553 at the John de Laeter Centre, Curtin University. MP, VP, EK, and DGS acknowledge support from the cooperative grant from the German Research Foundation (DFG)-Russian Foundation for Basic Research (RFBR) #GA1960/14-1 – #20-55-12011. SP was supported by the Russian Foundation for Basic Research, project 19-05-00743A. We acknowledge the help of A.S. Kumara, A. Frew, B. Ware, and E. Miller with mineral separation, zircon dissolution, solution ICP-MS analyses and SEM imaging. M. Thöner and U. Westernströer are thanked for their assistance with electron probe and LA-ICP-MS analyses. E. Garova, A. Zakharov, and N. Sychev are thanked for assistance in the field. S. Garipova is thanked for her help with design of the maps. I. Dunkl is thanked for sharing PepiFLEX software for ICP-MS data reduction. GEOMAR (Kiel, Germany) is thanked for funding the electron microprobe and thermal ionization mass spectrometry analyses. Constructive comments by B. Kohn and an anonymous reviewer helped to improve the manuscript; R. Hickey-Vargas is thanked for editorial handling.

Appendix A. Supplementary material

Supplementary material related to this article can be found online at https://doi.org/10.1016/j.epsl.2021.116890.

References

Akal, C., Helvacı, C., Prelević, D., van den Bogaard, P., 2013. High-K volcanism in the Afyon region, western Turkey: from Si-oversaturated to Si-undersaturated volcanism. Int. J. Earth Sci. 102, 435–453.

Aldanmaz, E., Pearce, J.A., Thirlwall, M.F., Mitchell, J.G., 2000. Petrogenetic evolution of late Cenozoic, post-collision volcanism in western Anatolia, Turkey. J. Volcanol. Geotherm. Res. 102, 67–95.

Aydar, E., et al., 2012. Correlation of ignimbrites in the central Anatolian volcanic province using zircon and plagioclase ages and zircon compositions. J. Volcanol. Geotherm. Res. 213–214, 83–97.

Chumakov, I.S., Byzova, L.S., Ganzei, S.S., 1992. Geochronology and Correlation of the Late Cenozoic Paratethys Deposits (Geokhronologiya i Korrelyatsiya Pozdnego Kainozoya Paratetisa). Nauka Publishers, Moscow. 96 p.

Danišík, M., et al., 2020. Sub-millennial eruptive recurrence in the silicic Mangaone Subgroup tephra sequence, New Zealand, from Bayesian modelling of zircon double-dating and radiocarbon ages. Quat. Sci. Rev. 246, 106517.

de Leeuw, A., et al., 2013. Paleomagnetic and chronostratigraphic constraints on the Middle to Late Miocene evolution of the Transylvanian Basin (Romania): Implications for Central Paratethys stratigraphy and emplacement of the Tisza–Dacia plate. Glob. Planet. Change 103, 82–98.

Dilek, Y., Imamverdiyev, N., Altunkaynak, Ş., 2010. Geochemistry and tectonics of Cenozoic volcanism in the Lesser Caucasus (Azerbaijan) and the peri-Arabian region: collision-induced mantle dynamics and its magmatic fingerprint. Int. Geol. Rev. 52 (4–6), 536–578.

Helvacı, C., et al., 2009. Geochemistry and $^{40}Ar/^{39}Ar$ geochronology of Miocene volcanic rocks from the Karaburun Peninsula: Implications for amphibole-bearing lithospheric mantle source, Western Anatolia. J. Volcanol. Geotherm. Res. 185, 181–202.

Hofmann, A.W., 2003. Sampling Mantle Heterogeneity Through Oceanic Basalts: Isotopes and Trace Elements. Trace Elements, Treatise on Geochemistry. Elsevier, pp. 61–101.

Iosifova, Yu.I., 1977. Geologic structure of the Miocene of the Oka-Don plain. In: Shik, S.M., Grichuk, V.P. (Eds.), Miocene of the Oka-Don Plain (Miocen Oksko-Donskoj Ravniny). Nedra, Moscow, pp. 6–52. In Russian.

Iosifova, Yu.I., 1992. On the age of the ash-bearing deposits in the Gorelka village (Voronezh region). In: Shik, S.M. (Ed.), Stratigraphy of the Phanerozoic Deposits of the East European Platform (Stratigrafiya Fanerozoya Centra Vostochno-Evropejskoj Platformy). Centrgeologiya, Moscow, pp. 36–59. In Russian.

Iosifova, Yu.I., Grishchenko, M.N., Krasnenkov, R.V., 1986. Northern part of the Central regions of the East European platform. In: Muratov, M.V., Nevesskaya, L.A. (Eds.), Stratigraphy of the USSR. Neogene System. (Stratigrafiya SSSR. Neogenovaya Sistema). Nedra, Moscow, pp. 308–331. In Russian.

Kiss, P., Gméling, K., Molnár, F., Pécskay, Z., 2010. Geochemistry of Sarmatian volcanic rocks in the Tokaj Mts (NE Hungary) and their relationship to hydrothermal mineralization. Central Europ. Geol. 53, 377–403.

Kovács, M., et al., 2017. Miocene volcanism in the Oaş–Gutâi Volcanic Zone, Eastern Carpathians, Romania: relationship to geodynamic processes in the Transcarpathian Basin. Lithos 294–295, 304–318.

Le Maitre, R.W., et al., 2002. Igneous rocks. In: A Classification and Glossary of Terms 2.

Le Pennec, J.L., et al., 2005. Stratigraphy and age of the Cappadocia ignimbrites, Turkey: reconciling field constraints with paleontologic, radiochronologic, geochemical and paleomagnetic data. J. Volcanol. Geotherm. Res. 141, 45–64.

Lebedev, V., Chernyshev, I., Sharkov, E., 2011. Geochronological scale and evolution of late Cenozoic magmatism within the Caucasian segment of the alpine belt. Dokl. Earth Sci. 441 (2), 1656–1660.

Lechmann, A., Burg, J.P., Ulmer, P., Guillong, M., Faridi, M., 2018. Metasomatized mantle as the source of Mid-Miocene-Quaternary volcanism in NW-Iranian Azerbaijan: geochronological and geochemical evidence. Lithos 304, 311–328.

Legros, F., 2000. Minimum volume of a tephra fallout deposit estimated from a single isopach. J. Volcanol. Geotherm. Res. 96, 25–32.

Lepetit, P., et al., 2014. $^{40}Ar/^{39}Ar$ dating of ignimbrites and plinian air-fall layers from Cappadocia, Central Turkey: implications to chronostratigraphic and Eastern Mediterranean palaeoenvironmental record. Geochemistry 74, 471–488.

Lowe, D.J., 2011. Tephrochronology and its application: a review. Quat. Geochronol. 6 (2), 107–153.

Ludwig, K.L., Mundil, R., 2002. Extracting reliable U-Pb ages and errors from complex populations of zircons from Phanerozoic tuffs. In: 12th Goldschmidt Conference, A-463. In: J. Conf. Abstracts.

Lukács, R., et al., 2018. Early to Mid-Miocene syn-extensional massive silicic volcanism in the Pannonian Basin (East-Central Europe): eruption chronology, correlation potential and geodynamic implications. Earth-Sci. Rev. 179, 1–19.

Lustrino, M., Wilson, M., 2007. The circum-Mediterranean anorogenic Cenozoic igneous province. Earth-Sci. Rev. 81 (1–2), 1–65.
Mason, P.R.D., et al., 1996. Crustal assimilation as a major petrogenetic process in the East Carpathian Neogene and Quaternary continental margin arc, Romania. J. Petrol. 37, 927–959.
Mason, P.R.D., Seghedi, I., Szákacs, A., Downes, H., 1998. Magmatic constraints on geodynamic models of subduction in the East Carpathians, Romania. Tectonophysics 297 (1–4), 157–176.
McDonough, W.F., Sun, S.S., 1995. The composition of the Earth. Chem. Geol. 120, 223–253.
Methner, K., et al., 2020. Middle Miocene long-term continental temperature change in and out of pace with marine climate records. Sci. Rep. 10 (1), 1–10.
Moghadam, H.S., et al., 2015. Petrogenesis and tectonic implications of Late Carboniferous A-type granites and gabbronorites in NW Iran: geochronological and geochemical constraints. Lithos 212, 266–279.
Ogg, J.G., 2020. Geomagnetic polarity time scale. In: Gradstein, F.M., Ogg, J.G., Schmitz, M.D., Ogg, G.M. (Eds.), The Geologic Time Scale 2020. Elsevier, Amsterdam, pp. 159–192.
Pearce, J.A., Peate, D.W., 1995. Tectonic implications of the composition of volcanic arc magmas. Annu. Rev. Earth Planet. Sci. 23, 251–285.
Pearce, J.A., Harris, N.B.W., Tindle, A.G., 1984. Trace-element discrimination diagrams for the tectonic interpretation of granitic-rocks. J. Petrol. 25, 956–983.
Pearce, J., et al., 1990. Genesis of collision volcanism in Eastern Anatolia, Turkey. J. Volcanol. Geotherm. Res. 44, 190–227.
Pearce, J., 1996. Sources and settings of granitic rocks. Episodes 19, 120–125.
Pécskay, Z., et al., 2006. Geochronology of Neogene magmatism in the Carpathian arc and intra-Carpathian area. Geol. Carpath. 57, 511.
Pécskay, Z., Seghedi, I., Downes, H., Prychodko, M., Mackiv, B., 2000. K/Ar dating of Neogene calc-alkaline volcanic rocks from Transcarpathian Ukraine. Geol. Carpath. 51 (2), 83–89.
Popov, S.V., et al., 2018. Stratotypes and reference sections of the Neogene regional stages of southern Russia and problems of their boundaries. In: Gladenkov, A.Y. (Ed.), Neogene and Quarter of Russia: Stratigraphy, Events and Paleogeography. (Neogen i Kvarter Rossii: Stratigrafiya, Sobytiya i Paleogeografiya). GEOS, Moscow, pp. 47–54. In Russian.
Popov, S.V., et al., 2004. Lithological-paleogeographic maps of Paratethys. In: Courer Forschungs Institut Senckenberg, Vol. 250, pp. 1–46.
Popov, S.V., Antipov, M.P., Zastrozhnov, A.S., Kurina, E.E., Pinchuk, T.N., 2010. Sea level fluctuations on the Northern shelf of the Eastern Paratethys in the Oligocene–Neogene. Stratigr. Geol. Correl. 18 (2), 200–224.
Portnyagin, M.V., et al., 2020. TephraKam: geochemical database of glass compositions in tephra and welded tuffs from the Kamchatka volcanic arc (northwestern Pacific). Earth Syst. Sci. Data 12 (1).
Pyle, D.M., 1995. Assessment of the minimum volume of tephra fall deposits. J. Volcanol. Geotherm. Res. 69, 379–382.
Pyle, D.M., et al., 2006. Wide dispersal and deposition of distal tephra during the Pleistocene 'Campanian Ignimbrite/Y5'eruption, Italy. Quat. Sci. Rev. 25 (21–22), 2713–2728.
Quan, C., Liu, Y.S.C., Tang, H., Utescher, T., 2014. Miocene shift of European atmospheric circulation from trade wind to westerlies. Sci. Rep. 4, 5660.
Rozsa, P., Elekes, Z., Gratuze, B., Uzonyi, I., Kiss, Á., 2006. Comparative geochemical studies of obsidian samples from various localities. Acta Geol. Hung. 49, 73–87.
Seghedi, I., et al., 2001. Magmagenesis in a subduction-related post-collisional volcanic arc segment: the Ukrainian Carpathians. Lithos 57, 237–262.
Szakács, A., et al., 2012. On the age of the Dej Tuff, Transylvanian Basin (Romania). Geol. Carpath. 63, 139–148.
Temel, A., Gündoğdu, M.N., Gourgaud, A., Le Pennec, J.-L., 1998. Ignimbrites of Cappadocia (Central Anatolia, Turkey): petrology and geochemistry. J. Volcanol. Geotherm. Res. 85, 447–471.
Vinogradov, A.P. (Ed.), 1967–1969. Atlas of the lithological-paleographical maps of the USSR. Ministry of Geology USSR, Moscow. 4 pts., 255 coloured maps.
Yakobovskaya, T.A., Iosifova, Yu.I., 1968. On the Miocene fauna of the Oka-Don plain. Dokl. Akad. Nauk SSSR 179 (6), 1424–1428. In Russian.
Zartman, R.E., Haines, S.M., 1988. The plumbotectonic model for Pb isotopic systematics among major terrestrial reservoirs – a case for bi-directional transport. Geochim. Cosmochim. Acta 52, 1327–1339.